Fat accumulates preferentially in the right rather than the left liver lobe in non-diabetic subjects

Bian, Hua

2018-02

Bian , H , Hakkarainen , A , Zhou , Y , Lundbom , N & Yki-Järvinen , H 2018 , ' Fat accumulates preferentially in the right rather than the left liver lobe in non-diabetic subjects ' , Digestive and Liver Disease , vol. 50 , no. 2 , pp. 168-174 . https://doi.org/10.1016/j.dld.2017.08.030

http://hdl.handle.net/10138/300965
https://doi.org/10.1016/j.dld.2017.08.030

publishedVersion

Digestive and Liver Disease 50 (2018) 168–174

Contents lists available at ScienceDirect

Digestive and Liver Disease

journal homepage: www.elsevier.com/locate/dld

Liver, Pancreas and Biliary Tract

Fat accumulates preferentially in the right rather than the left liver lobe in non-diabetic subjects

Hua Bian[a,b,*], Antti Hakkarainen[c], You Zhou[a,e], Nina Lundbom[c], Hannele Yki-Järvinen[a,d]

[a] Minerva Foundation Institute for Medical Research, Helsinki, Finland
[b] Department of Endocrinology, Zhongshan Hosipital, Fudan University, Shanghai, China
[c] Department of Radiology, Helsinki Medical Imaging Center, Helsinki University Central Hospital, University of Helsinki, Helsinki, Finland
[d] Department of Medicine, University of Helsinki, Helsinki, Finland
[e] Systems Immunity University Research Institute and Division of Infection and Immunity, School of Medicine, Cardiff University, Cardiff, United Kingdom

ARTICLE INFO

Article history:
Received 28 March 2017
Received in revised form 19 July 2017
Accepted 14 August 2017
Available online 23 August 2017

Keywords:
Insulin
Metabolic syndrome
Obesity

ABSTRACT

Aims: To examine the distribution of liver fat (LFAT) in non-diabetic subjects and test whether the fat in the right as compared to the left lobe correlates better with components of the metabolic syndrome or not.

Methods: In this cross sectional study, we determined LFAT by ^{1}H-MRS in the right lobe (LFAT%^{MRS}), and by MRI (LFAT%^{MRI}) in four regions of interest (ROIs 1–4, two in the right and two in the left lobe) in 97 non-diabetic subjects (age range 22–74 years, BMI 18–41 kg/m^2) and compared the accuracy of LFAT^{MRI} in the different ROIs in diagnosing non-alcoholic fatty liver disease (NAFLD) using areas under the receiver operator characteristic (AUROC) curves.

Results: 38% of the subjects had NAFLD (LFAT%^{MRS}). LFAT%^{MRI} was significantly higher in the right (5.7 ± 0.5%) than the left (5.1 ± 0.4%) lobe ($p < 0.02$). The AUROC for LFAT%^{MRI} in the right lobe for diagnosing NAFLD was significantly better than that in the left lobe. The relationships between several metabolic parameters and LFAT%^{MRI} in the left lobe were significantly worse than those for LFAT%^{MRS} while there was no difference between LFAT%^{MRS} and right lobe ROIs.

Conclusions: Liver right lobe contains more fat and correlates better with components of the metabolic syndrome than the left in non-diabetic subjects.

1. Introduction

Studies performed in dogs over 100 years ago showed that blood flow from the splenic vein streamlined to the left lobe of the liver, while blood from the superior mesenteric vein was directed to the right lobe [1,2]. Similarly, studies in humans have shown that blood from the superior mesenteric vein, which drains the right colon, ileum and jejunum, is directed to the right lobe while blood from the spleen and left colon drain to the left lobe [3]. In obese subjects, the rate of visceral lipolysis is increased compared to non-obese subjects and can account for up to 50% of free fatty acids (FFA) delivery to the liver [4]. Many obese subjects accumulate fat in the liver due to non-alcoholic causes (NAFLD) and therefore possibly an increased flux of FFA from visceral fat to the superior mesenteric vein. Studies using Doppler ultrasonography in healthy volunteers have shown that in response to a meal, intrahepatic portal vein blood flow increases more in the right than the left lobe [5]. FFA delivery from both the meal and from visceral lipolysis might preferentially increase liver fat content more in the right than the left lobe. Metabolic consequences of hepatic insulin resistance in NAFLD such as hyperinsulinemia and hypertriglyceridemia could therefore also be better correlated with fat in the right than the left lobe.

Few data are available examining fat distribution in the human liver. In an autopsy study, Merat et al. [6] analyzed three different parts of the liver (2 × 2 × 2 cm each) and found steatosis to be unevenly distributed (kappa = 0.64). Larson et al. [7] and Merriman et al. [8] took liver biopsies from the right and left lobes of morbidly obese patients and found low variability for steatosis between right and left lobes. However, multiple liver biopsies can not be used to assess heterogeneity of liver fat because of risks of bleeding.

Magnetic resonance imaging (MRI) methods enable accurate assessment of liver steatosis [9,10]. Until now, only one study has been published where heterogeneity of liver fat was analyzed in hospitalized patients with type 2 diabetes, who were using oral hypoglycaemic agents or insulin, and the right lobe was found

* Corresponding author at: Minerva Foundation Institute for Medical Research, University of Helsinki, Biomedicum 2U, Tukholmankatu 8, 00290 Helsinki, Finland. Fax: +358 9 191 25701.
E-mail address: bianhuaer@126.com (B. Hua).

https://doi.org/10.1016/j.dld.2017.08.030
1590-8658/

to contain more fat than the left lobe [11]. However, the pathways leading to NAFLD may differ between type 2 diabetic patients and non-diabetic subjects [12], and the drugs, especially insulin and glitazones could affect the routes which regulate intrahepatic fat content [13,14]. Regional variation in liver fat content in non-diabetic subjects has not been examined.

The liver is the source of glucose and (VLDL) triglycerides after an overnight fast, two of the key components of the metabolic syndrome. The liver, once fatty, becomes resistant to the normal actions of insulin to inhibit the production of glucose and VLDL [15]. This leads to hyperglycemia and stimulation of insulin secretion as well as hypertriglyceridemia [16]. All components of the metabolic syndrome are significantly correlated with liver fat content [15]. However, if there is, as discussed above, more fat in the right than the left lobe, the former might be better correlated with features of insulin resistance than the latter. Indeed, identification of the region, which best correlates with features of insulin resistance, could be considered as the region which physiologically defines the most relevant area of fat accumulation in the liver, and provides the area which enables the most accurate diagnosis of NAFLD.

In the present study, we hypothesized that the right lobe of the human liver would contain more fat than the left lobe in non-diabetic subjects, and that fat in the right as compared to the left lobe might correlate better with components of the metabolic syndrome. To this end, we quantified liver fat by MRI in 4 different regions of interest (ROIs) in 97 non-diabetic subjects, and also measured liver fat by proton magnetic resonance spectroscopy (^{1}H-MRS), the golden standard for measurement of liver fat content.

2. Methods

2.1. Subjects

We analyzed data from all non-diabetic subjects studied since August 2007 when we added an in-phase (IP) and out-of-phase (OP) imaging sequence to our MRI protocol to enable monitoring of spatial distribution of fat in the liver. This sequence covers the whole liver and allows to quantitate the intensity of the liver. The group comprised of 97 subjects (56 women, 41 men), who met the following inclusion criteria: i) age 20–75 years, ii) no known acute or chronic disease other than obesity, hypertension or NAFLD. iii) No evidence of advanced fibrosis as determined using the NAFLD fibrosis score [17]. Exclusion criteria included i) diabetes, ii) autoimmune liver disease (past medical history); iii) viral liver disease (positive for HBsAg or HCVAb), iv) drug-induced liver disease (past medical and drug use history), v) excessive use of alcohol (more than 20 g/day for men, more than 10 g/day in women [18]), vi) pregnancy or lactation. All protocols were in accordance with the Helsinki Declaration of 1975 and approved by the ethics committee of the Helsinki University Central Hospital, and each subject provided written informed consent.

Eligible subjects were studied after an overnight fast. At this visit, body weight and height, waist and hip circumferences were measured, % body fat and blood pressure were recorded, and blood samples were taken for measurement of biochemical parameters as detailed below. On a second occasion, ^{1}H-MRS and MRI studies were performed to quantitate liver fat (vide infra).

2.2. % liver fat (^{1}H-MRS)

Localised single voxel ($2 \times 2 \times 2$ cm^3) proton spectra were acquired using a 1.5-T whole-body system (Siemens Magnetom Avanto, Erlangen, Germany), which consisted of a combination of whole-body and loop surface coils for radiofrequency transmitting and signal receiving. T1- and T2-weighted high-resolution MR images were used for localisation of the voxel of interest within the right lobe of the liver. ^{1}H-MRS measurements of the liver fat were performed in the middle of the right lobe at a location that was individually determined for each subject by a single operator; vascular structures and subcutaneous fat tissue were avoided when selecting the voxel. Single voxel spectra were recorded using the point resolved spectroscopy (PRESS), with an echo time of 30 ms, a repetition time of 3000 ms, 1024 data points over 1000 kHz spectral width with 16 averages. A short echo time and long repetition time were chosen to ensure a fully relaxed water signal, which was used as an internal standard. Chemical shifts were measured relative to water at 4.70 ppm. The methylene signal, which represents intracellular triglyceride, was measured at 1.3 ppm. Signal intensities were quantified by using a jMRUI v3.0 analysis program [19] with an advanced method for accurate, robust and efficient spectral fitting (AMARES) [20]. Signal intensities were corrected for T2 relaxation as previously described [21]. Spectroscopic intracellular triglyceride content (LFAT) was expressed as a ratio of the area under the methylene peak to that under the methylene and water peaks. LFAT% was converted from signal ratios to volume fractions by applying the method validated by Longo et al. [22] and using experimentally determined values by Szczepaniak et al. [23] ($\times 100$ = % liver fat). This measurement has been validated against histologically determined lipid content [24] and against estimates of fatty degeneration or infiltration by X-ray computer-assisted tomography by us [25] and others [26]. All spectra were analysed by a physicist who was unaware of any of the clinical data. The reproducibility of repeated measurements of LFAT in non-diabetic subjects studied on two occasions in our laboratory is 11%. NAFLD was defined as in the population-based Dallas Heart Study, as a LFAT% > 5.55% [27].

2.3. Liver fat fraction (MRI)

A body coil was used to obtain coronal scout images of the upper abdomen. A stack of transaxial IP and OP T1-weighted dual-echo fast spoiled-gradient recalled images were obtained in two breath holds using following imaging parameters: 103 ms repetition time, 2.12 ms (OP)/4.8 ms (IP) echo time, 80° flip angle, 24 slices ($\times 2$), 1 cm slice thickness, 512×448 matrix and 5 dm $\times$ 4.37 dm field of view, the same matrix and field was used for all patients. Transaxial abdominal scans encompassing the entire liver were acquired in two breath-holds using the magnet mentioned above. Each 2D slice was displayed on the video screen. Using the Image J 1.46r software to analyze the intensity of the liver, four ROIs (1–2 cm in diameter) were obtained in the liver above the portal vein (two in the right lobe and two in the left lobe, Fig. 1). ROIs 1–4 were located in liver segments II, IV, VIII, VII, respectively. The standard deviation of the signal intensity measure ements within each ROI was kept to less than 10%. The ROIs included areas of parenchyma that did not contain vessels or artifacts, and the ROIs were in corresponding locations in the paired IP and OP MR images. The signal intensity of the spleen was measured as the mean intensity from the three 1 to 2 cm ROIs (Fig. 1). LFATFr^{MRI} was quantified on T1-weighted dual-echo gradient-echo MR images as the percentage of relative signal intensity loss of the liver on OP images, with the following formula: $(SI_{in} - SI_{out})/SI_{in} \times 100$, where SI is the mean liver signal intensity divided by the mean spleen signal intensity, SI_{in} is IP signal intensity, and SI_{out} is OP signal intensity [10]. LFATFr^{MRI} was converted to ^{1}H-MRS % units (% liver fat by MRI, LFAT%^{MRI}) using the equation relating MRI and ^{1}H-MRS measurements (see Section 3).

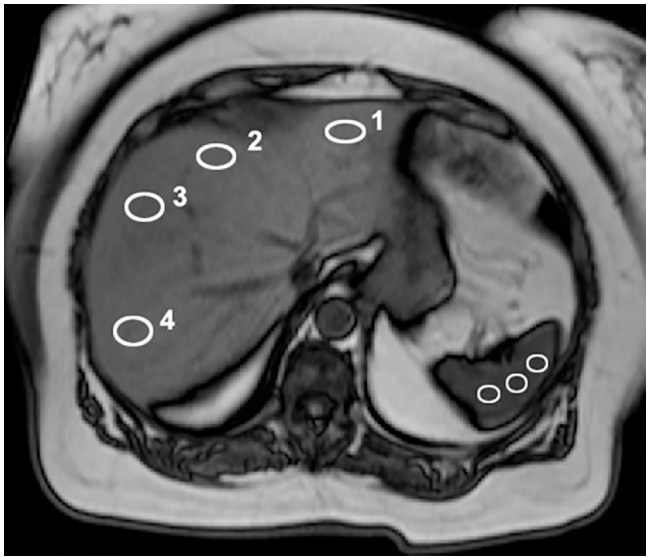

Fig. 1. Positions of region of interests (ROIs) 1–4 in the liver and 3 ROIs in the spleen on T1-weighted dual-echo gradient-echo sequence. ROIs 3, 4 were in the right and ROIs 1, 2 in the left hepatic lobe. ROIs 1–4 belong to liver segment II, IV, VIII, VII, respectively.

2.4. Intra-abdominal fat and subcutaneous fat (MRI)

A series 16 of T1-weighted axial images with selective fat excitation were acquired from a region extending from 8 cm above to 8 cm below the L4/5 lumbar intervertebral disks (16 slices, field of view $438 \times 500\ mm^2$, slice thickness 1 cm, breath-hold repetition time 91 ms, echo time 5.24 ms). Intra-abdominal and subcutaneous fat areas for each slice were determined using a region growing method in SliceOmatic v4.3 image analysis program (Tomovision, Montreal, Canada). The areas were multiplied by the slice thickness and the results were expressed as total volumes of Intra-abdominal and subcutaneous adipose tissues [25].

2.5. Other measurements and analytical procedures

Waist circumference was measured midway between the spinailiaca superior and the lower rib margin, and hip circumference at the level of the greater trochanters [28]. Body weight was recorded to the nearest 0.1 kg using a calibrated weighting scale (Soehnle, Monilaite-Dayton, Finland) with subjects barefoot and wearing light indoor clothing. Body height was recorded to the nearest 0.5 cm using a ruler attached to the scale. % body fat was determined by bioimpedance plethysmography as previously described [29].

Blood pressure was measured in the sitting position after 10–15 min of rest using a random-zero sphygmomanometer (Erka, Germany). Fasting plasma glucose (FPG) concentrations were measured in duplicate using the glucose oxidase method using Beckman Glucose Analyzer II (Beckman Instruments, Fullerton, CA) [30]. Fasting serum (fS) free insulin concentrations were measured with the Auto-DELFIA kit (Wallac, Turku, Finland). Glycosylated hemoglobin A_{1c} (HbA_{1c}) was measured by high performance liquid chromatography using the fully automated Glycosylated Haemoglobin Analyzer System (BioRad, Richmond, CA) [31]. Serum (S) total cholesterol, high density lipoprotein (HDL) cholesterol and triglyceride concentrations were measured with the enzymatic kits from Roche Diagnostics using an auto-analyser (Roche Diagnostics Hitachi, Hitachi Ltd., Tokyo, Japan). The concentrations of low density lipoprotein (LDL) cholesterol were calculated using the Friedewald formula [32]. Serum albumin, blood counts, alanine aminotransferase (ALT), aspartate aminotransferase (AST) and gamma-glutamyltransferase (GGT) activities were determined as recommended by the European Committee for Clinical Laboratory Standards. The NAFLD fibrosis score was calculated as described by Angulo et al. [17] and as recommended by the American College of Gastroenterology [33]. Serum hepatitis B virus surface antigen (HBsAg) and hepatitis C virus antibody (HCV-Ab) were tested by the Enhanced Electrochemiluminescence method.

Homeostasis model assessment-insulin resistance (HOMA-IR) was calculated as described by Matthews et al. [34].

2.6. Statistical analyses

Normal distribution of data was analyzed using the Kolmogorov–Smirnov test. Non-normally distributed data were used after logarithmic (base 10) transformation. Normally distributed data are shown as mean ± SE, whereas non-normally distributed data are shown as median followed by the 25% and 75% percentiles. The unpaired Student's t-test and the Mann–Whitney test were used to compare mean values of normally and non-normally distributed data. Pearson's correlation coefficient was calculated for normally and Spearman's rank correlation coefficient for non-normally distributed data. Lin's concordance coefficient, which combines measurements of precision and accuracy, was computed to determine whether the observed data deviate significantly from the line of perfect agreement [35]. Multiple linear regression analysis was performed to set an equation to get the $LFAT\%^{MRI}$ from $LFATFr^{MRI}$ using $LFAT\%^{MRS}$ as reference standard and test which part of $LFAT\%^{MRI}$ was the independent predictor of $LFAT\%^{MRS}$. Correlation coefficients were compared using the Hotelling–Williams test by R 2.13.1 statistical package (R software, R Foundation for Statistical Computing, Vienna, Austria). Receiver operating characteristic (ROC) curves were set up by SPSS 20.0 for Windows (SPSS, Chicago, IL) and compared using the Medcalc 12.7.1.0 (MedCalc Software, Mariakerke, Belgium). Values of area under receiver operating characteristic (AUROC) equalling 1 represent a perfect test; between 0.9 and 1 were considered as excellent; between 0.8 and 0.9 good; between 0.7 and 0.8 fare; between 0.6 and 0.7 poor; and 0.5 a worthless test. Other calculations were made using SPSS 20.0 for Windows and GraphPad Prism version 5.00 for Windows (GraphPad Software, San Diego, CA). A p-value of less than 0.05 was considered statistically significant.

3. Results

3.1. Characteristics of the study subjects

Anthropometric and biochemical characteristics of the subjects are summarized in Table 1. 38% of the subjects had NAFLD as measured by $LFAT\%^{MRS}$. None of the subjects had evidence of fibrosis (NAFLD fibrosis score <0.676 [17]). The $LFAT\%^{MRS}$ averaged 5.8 ± 0.6% (1.9 ± 0.2% for non-NAFLD, 12.0 ± 0.7% for NAFLD, $p < 0.001$).

3.2. Regional variation in liver fat

The equation relating $LFAT\%^{MRS}$ (right lobe) and $LFATFr^{MRI}$ (right lobe) was as follows: $LFAT\%^{MRS} = (2.837 \pm 0.374) + (0.198 \pm 0.013) \times LFATFr^{MRI}$ ($r = 0.837$, $p < 0.001$, Fig. 2). $LFAT\%^{MRI}$ in ROIs 1, 2, 3 and 4 averaged: 4.8 ± 0.5%, 5.5 ± 0.5%, 5.8 ± 0.5% and 5.7 ± 0.5%. The $LFAT\%^{MRI}$ was significantly lower in ROI 1 than in ROI 2 ($p < 0.02$), ROI 3 ($p < 0.001$) and ROI 4 ($p < 0.02$, Fig. 3). $LFAT\%^{MRI}$ was significantly higher in the right (5.7 ± 0.5%) than the left (5.1 ± 0.4%) lobe ($p < 0.02$, Fig. 3).

The correlation coefficients (Pearson) between $LFAT\%^{MRS}$ and $LFATFr^{MRI}$ in ROIs were: $r = 0.738$, $p < 0.001$ for ROI 1, $r = 0.785$,

Table 1
Anthropometric and biochemical characteristics of the subjects.

	Total (n = 97)	Non-NAFLD (n = 60)	NAFLD (n = 37)
Age (year)	51 ± 1	49 ± 2	54 ± 2*
Weight (kg)	83.6 ± 1.8	77.9 ± 2.0	92.2 ± 2.9***
Body mass index (kg/m^2)	28.3 ± 0.5	26.6 ± 0.6	31.0 ± 0.8***
Waist circumference (cm)	94.9 ± 1.6	89.9 ± 1.9	102.7 ± 2.2***
Hip circumference (cm)	104.7 ± 1.1	101.3 ± 1.2	110.1 ± 1.8***
Waist-to-hip-ratio	0.90 ± 0.01	0.88 ± 0.01	0.93 ± 0.01**
Fasting plasma glucose (mmol/l)	5.4 ± 0.1	5.2 ± 0.1	5.8 ± 0.1***
fS-insulin (mU/l)	6.1 (3.5–12.5)	4.6 (2.7–7.1)	12.0 (6.7–14.7)***
HOMA-IR	1.42 (0.84–3.09)	0.98 (0.60–1.70)	2.87 (1.68–3.74)***
fS-triglycerides (mmol/l)	1.10 (0.74–1.57)	0.89 (0.70–1.29)	1.36 (0.93–1.86)**
fS-HDL cholesterol (mmol/l)	1.44 ± 0.04	1.57 ± 0.06	1.26 ± 0.05**
fS-LDL cholesterol (mmol/l)	3.07 ± 0.08	3.07 ± 0.10	3.06 ± 0.15
S-ALT (U/L)	29 (22–44)	24 (17–32)	45 (35–66)
S-AST (U/L)	30 (25–35)	26 (23–31)	35 (30–43)
S-GGT (U/L)	24 (16–44)	19 (13–28)	36 (24–60)
NAFLD fibrosis score	−2.19 ± 1.31	−2.36 ± 1.17	−1.98 ± 1.47
NAFLD fibrosis score%[a]	0	0	0

Abbreviations: NAFLD, non-alcoholic fatty liver disease; fS, fasting serum; HOMA-IR, homeostasis model assessment-insulin resistance; S, serum; ALT, alanine aminotransferase; AST, aspartate aminotransferase; GGT, gamma-glutamyltransferase; HDL, high density lipoprotein; LDL, low density lipoprotein. Data are shown as mean ± SE or median (25% percentile, 75% percentile).

* p < 0.05.
** p < 0.02.
*** p < 0.001 for vs. non-NAFLD.
[a] Patients with advanced fibrosis (NAFLD fibrosis score >0.676).

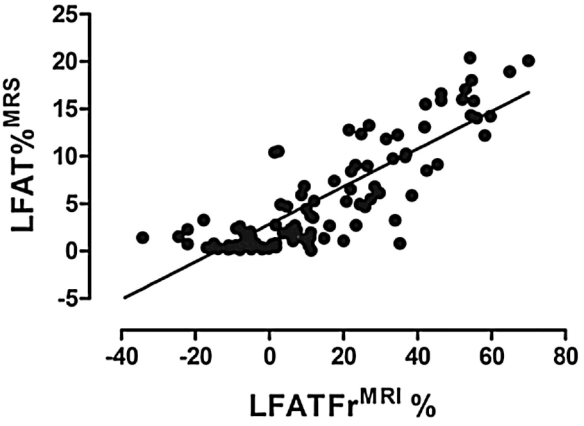

Fig. 2. Correlation between % liver fat by proton magnetic resonance spectroscopy (LFAT%^{MRS}) and liver fat fraction by magnetic resonance imaging (LFATFr^{MRI}). LFATFr^{MRI} in the right lobe was closely correlated with LFAT%^{MRS} (r = 0.837, p < 0.001).

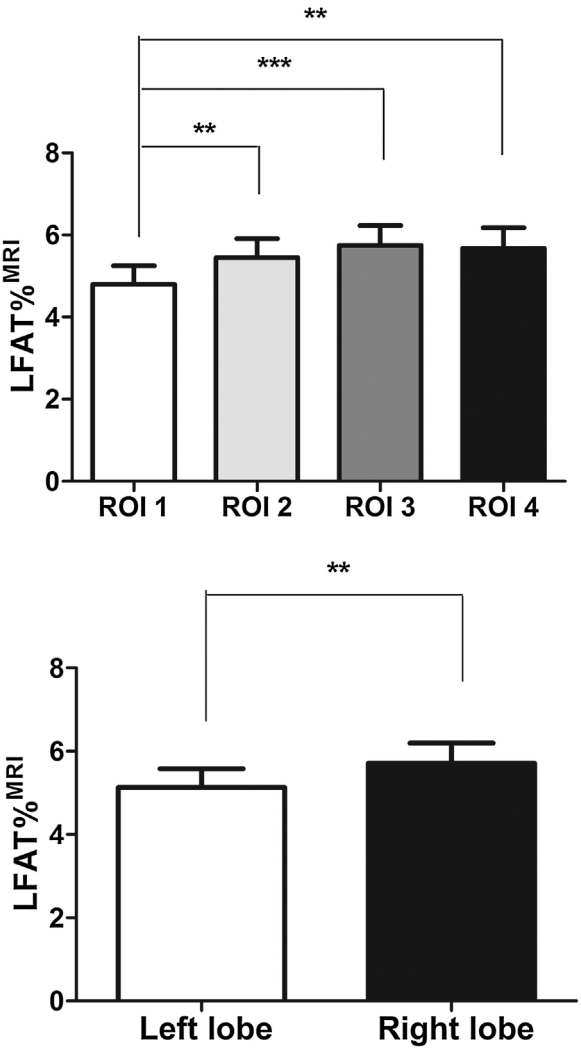

Fig. 3. % liver fat by magnetic resonance imaging (LFAT%^{MRI}) in different region of interests (ROIs). Data are shown as mean ± SE. **p < 0.02, ***p < 0.001.

p < 0.001 for ROI 2, r = 0.825, p < 0.001 for ROI 3, r = 0.828, p < 0.001 for ROI 4; r = 0.837, p < 0.001 for the right lobe and r = 0.781, p < 0.001 for the left lobe. Lin's concordance coefficients between LFAT%^{MRS} and LFAT%^{MRI} in ROIs were: rho(c) = 0.704, p < 0.001 for ROI 1, rho(c) = 0.763, p < 0.001 for ROI 2, rho(c) = 0.808, p < 0.001 for ROI 3, and rho(c) = 0.820, p < 0.001 for ROI 4, rho(c) = 0.824, p < 0.001 for the right lobe, rho(c) = 0.74, p < 0.001 for the left lobe.

Multiple linear regression analysis showed LFAT%^{MRI} in the right but not the left lobe was an independent predictor of LFAT%^{MRS} (β = 0.160, p < 0.001).

We analyzed ROC curves to determine how use of different ROIs influence the diagnosis of NAFLD. LFAT%^{MRI} in ROI 3 showed excellent accuracy in diagnosing NAFLD (AUROC = 0.936 ± 0.023, p < 0.001, sensitivity 94.6%, specificity 83.3%). The AUROC for ROI 1 was good (AUROC = 0.879 ± 0.034, p < 0.001, sensitivity 70.3%, specificity 90.0%) but significantly lower than that of AUROC for ROI 3 (p < 0.02; Table 2). Likewise, the AUROC was significantly higher using LFAT%^{MRI} in the right (AUROC = 0.934 ± 0.025, p < 0.001, sensitivity 86.5%, specificity 90.0%) than in the left lobe (AUROC = 0.894 ± 0.032, p < 0.001, sensitivity 73.0%, specificity 91.7%) lobe (p < 0.05, Table 2, Fig. 4).

Table 2
ROC curves to diagnose the NAFLD using LFAT%^{MRI} in different ROIs.

	AUROC	SE	p value for AUROC	Sensitivity %	Specificity %	PPV %	NPV %	Youden index
ROI 1	0.879	0.034	<0.001	70.3	90.0	81.3	83.0	0.603
ROI 2	0.894	0.032	<0.001	83.8	78.3	70.5	88.7	0.621
ROI 3	0.936**,††	0.023	<0.001	94.6	83.3	77.8	96.2	0.779
ROI 4	0.930	0.029	<0.001	89.2	90.0	84.6	93.1	0.792
Right lobe	0.934*,†,§	0.025	<0.001	86.5	90.0	84.2	91.5	0.765
Left lobe	0.894‡‡	0.032	<0.001	73.0	91.7	84.4	84.6	0.647

Abbreviations: ROC, receiver operating characteristic; NAFLD, non-alcoholic fatty liver disease; ROI, region of interest; AUROC, area under the receiver operating characteristic; PPV, positive predictive value; NPV, negative predictive value.
* p < 0.05.
** p < 0.02 for vs. ROI 1.
† p < 0.05.
†† p < 0.02 for vs. ROI 2.
‡‡ p < 0.02 for vs. ROI 3.
§ p < 0.05 for vs. left lobe.

Table 3
Correlation coefficients between metabolic parameters and LFAT%^{MRS} or LFAT%^{MRI} in different ROIs.

		LFAT%^{MRI}						
	LFAT%^{MRS}	Mean (ROIs 1–4)	ROI 1	ROI 2	ROI 3	ROI 4	Left lobe	Right lobe
Body mass index	0.577***	0.441***	0.366***,†	0.412***	0.469***	0.429***	0.404***	0.454***
Waist circumference	0.624***	0.503***	0.417***,†	0.488***	0.545***	0.494***	0.465***	0.525***
Hip circumference	0.539***	0.400***	0.297**,†	0.391***	0.446***	0.401***	0.344***,†	0.428***
Waist-to-hip-ratio	0.470***	0.404***	0.386***	0.378***	0.419***	0.378***	0.400***	0.403***
Fasting plasma glucose	0.467***	0.352***	0.269**	0.297**	0.383***	0.404***	0.298**	0.396***
HBA1c	0.445***	0.477***	0.424***	0.464***	0.482***	0.491***	0.449***	0.493***
fS-insulin	0.615***	0.518***	0.468***	0.450***	0.512***	0.537***	0.477***	0.534***
HOMA-IR	0.618***	0.543***	0.457***	0.447***,†	0.516***	0.543***	0.469***	0.539***
fS-triglyceride	0.547***	0.431***	0.387***	0.384***	0.429***	0.422***	0.406***	0.427***
fS-HDL cholesterol	−0.391***	−0.377***	−0.398***	−0.337***	−0.335***	−0.360***	−0.381***	−0.355***
S-AST	0.556***	0.409***	0.332***,†	0.356***,†	0.444***	0.438***	0.364***,†	0.440***
S-ALT	0.708***	0.574***	0.504***,††	0.502***,††	0.594***	0.604***	0.527***,†	0.604***
S-GGT	0.548***	0.446***	0.411***	0.409***	0.473***	0.440***	0.434***	0.454***
Body fat (%)	0.348***	0.249**	0.108†	0.221*	0.310**	0.286**	0.167	0.308**
Intra-abdominal fat	0.668*,**	0.598***	0.511***,†	0.579***	0.614***	0.574*,***	0.554***	0.604***
Subcutaneous fat	0.521***	0.427***	0.295**,†	0.406***	0.485***	0.453***	0.343**	0.479***

Abbreviations: LFAT%^{MRS}, % liver fat by proton magnetic resonance spectroscopy; LFAT%^{MRI}, % liver fat by magnetic resonance imaging; ROI, region of interest; fS, fasting serum; HBA1c, glycosylated hemoglobin A_{1c}; HDL, high density lipoprotein; S, serum; AST, aspartate aminotransferase; ALT alanine aminotransferase; GGT, gamma-glutamyltransferase. Hotelling–Williams test to compare r-values for the relationship between LFAT%^{MRS} or LFAT%^{MRI} in different ROIs and given metabolic parameters.
* p < 0.05.
** p < 0.02.
*** p < 0.001 for r-values.
†† p < 0.05 for LFAT%^{MRI} in different ROIs vs. LFAT%^{MRS}.

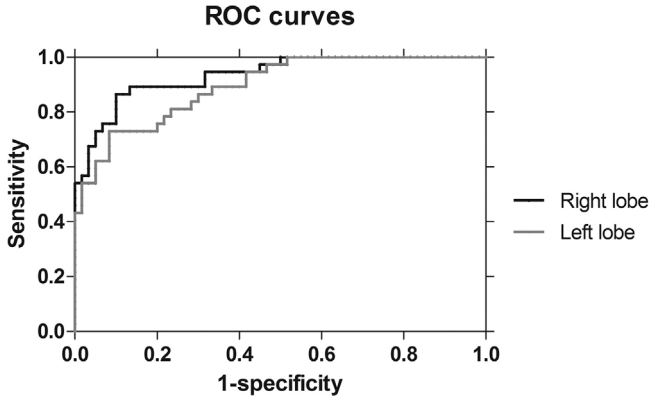

Fig. 4. Receiver operating characteristic (ROC) curves to diagnose the non-alcoholic fatty liver disease using % liver fat by magnetic resonance imaging (LFAT%^{MRI}) in the right and left lobe. Area under receiver operating characteristic (AUROC) was significantly higher using LFAT%^{MRI} in the right (AUROC = 0.934 ± 0.025, p < 0.001, sensitivity 86.5%, specificity 90.0%) rather than in the left (AUROC = 0.894 ± 0.032, p < 0.001, sensitivity 73.0%, specificity 91.7%) lobe.

3.3. Metabolic parameters and liver fat in different ROIs

The relationships between metabolic parameters and LFAT%^{MRS} and LFAT%^{MRI} in the different ROIs are shown in Table 3. The correlation coefficients between BMI, waist and hip circumference, body fat, intra-abdominal and subcutaneous fat, S-AST, S-ALT and LFAT%^{MRS} were significantly higher than those between these metabolic features and LFAT%^{MRI} in ROI 1 (Fig. 5, Table 3). The correlation coefficient between HOMA-IR, S-AST, S-ALT and LFAT%^{MRI} in ROI 2 was significantly lower than those between LFAT%^{MRS} and these metabolic features (Fig. 5, Table 3). The correlation coefficients between the metabolic parameters and LFAT%^{MRI} in ROIs 3 and 4 did not differ from those relating the respective parameters and LFAT%^{MRS} (Fig. 5, Table 3).

4. Discussion

In the present study of 97 non-diabetic subjects, we found the right lobe of the liver to contain significantly more fat than the left lobe. Measurement of liver fat in the right lobe perhaps provided a significantly more accurate diagnosis of NAFLD than that in the left lobe. Since liver fat was not homogenously distributed, we examined, which region in the liver was most closely associated with metabolic abnormalities associated with NAFLD. The correlation coefficients for measures of obesity, liver enzymes and HOMA-IR were best associated with fat in the right lobe of the liver. The right lobe could therefore be recommended as the location for quantification of liver fat in diagnosing NAFLD.

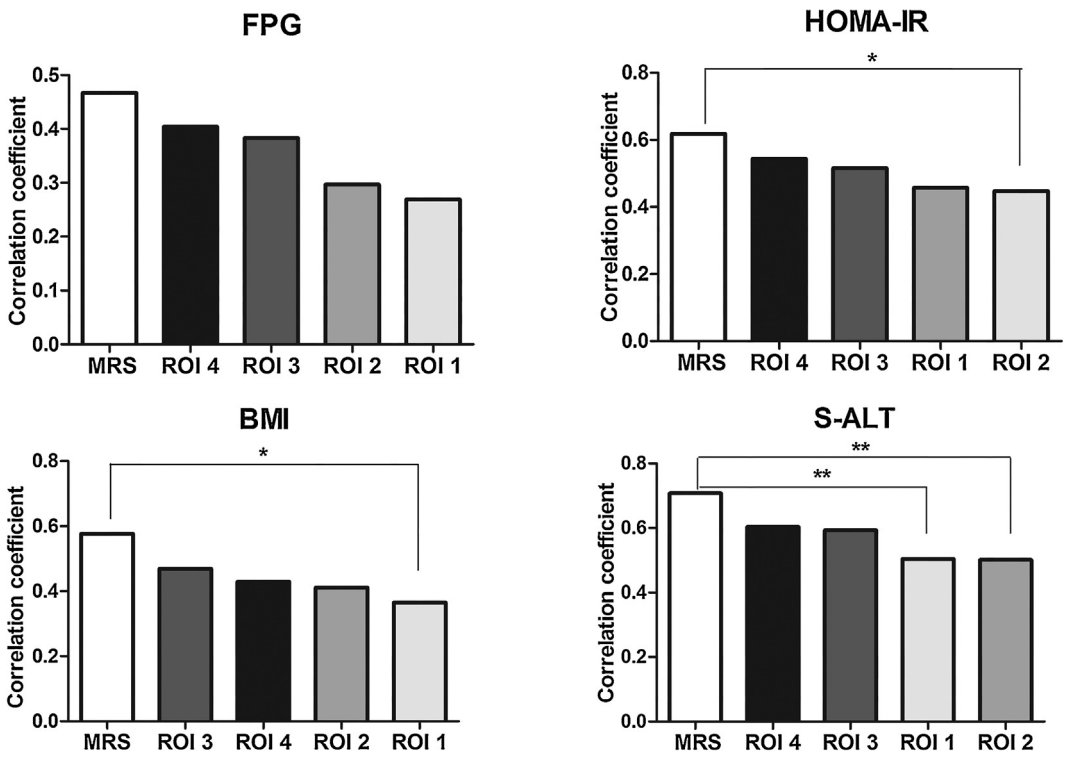

Fig. 5. The relationships between metabolic parameters andproton magnetic resonance spectroscopy (LFAT%^{MRS}) or % liver fat by magnetic resonance imaging (LFAT%^{MRI}) in different region of interests (ROIs). The Hotelling–Williams test was used to compare r-values for the relationship between LFAT%^{MRS}(white bar) or LFAT%^{MRI} in different ROIs (grey or black bars) and given metabolic parameters, *$p < 0.05$, **$p < 0.02$.FPG, fasting plasma glucose; HOMA-IR, homeostasis model assessment-insulin resistance; BMI, body mass index; S-ALT, serum alanine aminotransferase.

Compared to ^{1}H-MRS, MRI is available on most MR units and can be performed easily in routine examinations [36]. Previous studies have shown that MRI-based measurements of the liver fat are closely correlated with those obtained by ^{1}H-MRS [9,37]. These studies included patients with type 2 diabetes (n = 33) and those with a fatty liver (n = 12), and found the correlation coefficient between MRI and ^{1}H-MRS methods to be 0.959 [9] and 0.950 [37]. The correlation coefficient found in the present study in 97 subjects (0.837) is in line with these data.

Distribution of liver fat has been analysed using MRI or MRS in only one study [11]. In the study of Captan et al. in hospitalized type 2 diabetic patients, liver fat averaged 8.9% in the right and 7.7% in the left lobe ($p < 0.001$). The present data in non-diabetic subjects showed a similar difference in the fat content of the liver lobes as Captan et al. [11].

The present study does not provide mechanistic insights as to why liver fat content is significantly higher in the right than the left lobe. The most probable explanation is provided by previous data showing that portal blood flow is streamline rather than turbulent. Portal blood flow conveyed via the superior mesenteric vein drains visceral fat and supplies the right lobe of the liver while blood from the spleen flows into the left lobe [1,2]. Fat does not accumulate in the spleen in obesity [38,39]. In keeping with these data on blood flow and on the increased visceral lipolysis in obesity [4], we found waist circumference and visceral fat to correlate better with fat in the right than the left lobe. Dauzat et al. measured the hemodynamic effects of a meal on the splanchnic and hepatic circulation in 30 healthy volunteers using Doppler ultrasonography [5]. Intrahepatic portal blood flow was shown to increase significantly more in the right than the left lobe [5]. Thus, the right lobe may receive more substrates for hepatic lipogenesis such as fatty acids, glucose and amino acid also postprandially. Direct measurement of blood flow distribution in the liver of patients with NAFLD combined with quantification of the contribution of different pathways (lipolysis, de novo lipogenesis, the spillover pathways, uptake of chylomicron remnants postprandially) would be needed to provide mechanistic insights for the present data.

The present data are to our knowledge the first to relate metabolic features of NAFLD to fat content of different regions of the liver. Given the heterogeneous distribution of liver fat, such analysis is of interest as it helps to identify the region of the liver, which should be used for diagnosis of NAFLD. We found the correlation coefficients between LFAT%^{MRI} in ROI 3 and ROI 4 and measures of both subcutaneous and visceral obesity to be as good as those between these measures and LFAT%^{MRS}. The correlation coefficient between LFAT%^{MRI} in ROI 1 was worse than that between the measures of obesity and LFAT%^{MRS}. These data suggest that obesity increases liver fat especially in the right lobe of the liver. Liver enzymes, a simple but not ideal marker of NAFLD and non-alcoholic steatohepatitis (NASH) [40], were also better correlated with liver fat in the right lobe. Finally, HOMA-IR, a product of fasting insulin and glucose, was significantly worse correlated with LFAT%^{MRI} in ROI 2 but not the other ROIs than with LFAT%^{MRS}. These data suggest that fat accumulates in the right region of the liver and that this may correlate better with insulin resistance and metabolic abnormalities than the left.

One limitation of our study was only addressed to evaluate the relative distribution of liver fat into the right and the left lobe and its association with metabolic abnormalities, but not addressed to explore the relationship between the liver fat distribution and the severity of liver damage. Accordingly, no insights about this relationship should be provided. Another shortc oming was that we did not offer much mechanism as to heterogeneity of liver fat that should be further studied in the future.

5. Conclusion

In conclusion, liver fat is heterogeneously distributed in non-diabetic subjects, right lobe containing more fat than the left. When measured by MRI as in the present study, quantification of fat in the right as compared to the left lobe perhaps allows a more accurate diagnosis of NAFLD (Fig. 4). Metabolic abnormalities including obesity, liver enzymes and insulin resistance are also closer associated with fat in the right than in the left lobe (Table 3, Fig. 5). Quantification of liver fat in the right lobe may become of increasing clinical interest by ultrasound techniques or in conjunction with abdominal MRI performed for other indications. The study results are preliminary and need to be reproduced in a larger sample size and validated.

Conflict of interest

None declared.

Disclosure statement

The authors have nothing to disclose.

Acknowledgements

We gratefully acknowledge Anne Salo, Katja Sohlo and Mia Urjansson (Helsinki University Central Hospital, Department of Medicine) as well as Pentti Pölönen (Helsinki University Central Hospital, Department of Radiology) for skilful technical assistance.

References

[1] Serege H. Contribution a l'etude de la circulation du sang porte dans le foie et des localizations lobaires hepatiques. Journal de Medecine de Bordeaux 1901;31:271–5, 91–95, 312–314.
[2] Bartlett F, Corper H, Long E. The independence of the lobes of the liver. Am J Physiol 1914;35:36–50.
[3] Gates GF, Dore EK. Streamline flow in the human portal vein. J Nucl Med 1973;14:79–83.
[4] Nielsen S, Guo Z, Johnson CM, et al. Splanchnic lipolysis in human obesity. J Clin Invest 2004;113:1582–8.
[5] Dauzat M, Lafortune M, Patriquin H, et al. Meal induced changes in hepatic and splanchnic circulation: a noninvasive Doppler study in normal humans. Eur J Appl Physiol Occup Physiol 1994;68:373–80.
[6] Merat S, Sotoudehmanesh R, Nouraie M, et al. Sampling error in histopathology findings of nonalcoholic fatty liver disease: a post mortem liver histology study. Arch Iran Med 2012;15:418–21.
[7] Larson SP, Bowers SP, Palekar NA, et al. Histopathologic variability between the right and left lobes of the liver in morbidly obese patients undergoing Roux-en-Y bypass. Clin Gastroenterol Hepatol 2007;5:1329–32.
[8] Merriman RB, Ferrell LD, Patti MG, et al. Correlation of paired liver biopsies in morbidly obese patients with suspected nonalcoholic fatty liver disease. Hepatology 2006;44:874–80.
[9] Borra RJ, Salo S, Dean K, et al. Nonalcoholic fatty liver disease: rapid evaluation of liver fat content with in-phase and out-of-phase MR imaging. Radiology 2009;250:130–6.
[10] Qayyum A, Goh JS, Kakar S, et al. Accuracy of liver fat quantification at MR imaging: comparison of out-of-phase gradient-echo and fat-saturated fast spin-echo techniques—initial experience. Radiology 2005;237:507–11.
[11] Capitan V, Petit JM, Aho S, et al. Macroscopic heterogeneity of liver fat: an MR-based study in type-2 diabetic patients. Eur Radiol 2012;22:2161–8.
[12] Kotronen A, Juurinen L, Hakkarainen A, et al. Liver fat is increased in type 2 diabetic patients and underestimated by serum alanine aminotransferase compared with equally obese nondiabetic subjects. Diabetes Care 2008;31:165–9.
[13] Juurinen L, Tiikkainen M, Hakkinen AM, et al. Effects of insulin therapy on liver fat content and hepatic insulin sensitivity in patients with type 2 diabetes. Am J Physiol Endocrinol Metab 2007;292:E829–35.
[14] Yki-Jarvinen H. Thiazolidinediones. N Engl J Med 2004;351:1106–18.
[15] Kotronen A, Yki-Jarvinen H. Fatty liver: a novel component of the metabolic syndrome. Arterioscler Thromb Vasc Biol 2008;28:27–38.
[16] Kotronen A, Seppanen-Laakso T, Westerbacka J, et al. Hepatic stearoyl-CoA desaturase (SCD)-1 activity and diacylglycerol but not ceramide concentrations are increased in the nonalcoholic human fatty liver. Diabetes 2009;58:203–8.
[17] Angulo P, Hui JM, Marchesini G, et al. The NAFLD fibrosis score: a noninvasive system that identifies liver fibrosis in patients with NAFLD. Hepatology 2007;45:846–54.
[18] Bhala N, Usherwood T, George J. Non-alcoholic fatty liver disease. BMJ 2009;339:b2474.
[19] Naressi A, Couturier C, Castang I, et al. Java-based graphical user interface for MRUI, a software package for quantitation of in vivo/medical magnetic resonance spectroscopy signals. Comput Biol Med 2001;31:269–86.
[20] Vanhamme L, van den Boogaart A, Van Huffel S. Improved method for accurate and efficient quantification of MRS data with use of prior knowledge. J Magn Reson 1997;129:35–43.
[21] Kotronen A, Peltonen M, Hakkarainen A, et al. Prediction of non-alcoholic fatty liver disease and liver fat using metabolic and genetic factors. Gastroenterology 2009;137:865–72.
[22] Longo R, Pollesello P, Ricci C, et al. Proton MR spectroscopy in quantitative in vivo determination of fat content in human liver steatosis. J Magn Reson Imaging 1995;5:281–5.
[23] Szczepaniak LS, Babcock EE, Schick F, et al. Measurement of intracellular triglyceride stores by H spectroscopy: validation in vivo. Am J Physiol 1999;276:E977–89.
[24] Thomsen C, Becker U, Winkler K, et al. Quantification of liver fat using magnetic resonance spectroscopy. Magn Reson Imaging 1994;12:487–95.
[25] Ryysy L, Hakkinen AM, Goto T, et al. Hepatic fat content and insulin action on free fatty acids and glucose metabolism rather than insulin absorption are associated with insulin requirements during insulin therapy in type 2 diabetic patients. Diabetes 2000;49:749–58.
[26] Lukaski HC, Johnson PE, Bolonchuk WW, et al. Assessment of fat-free mass using bioelectrical impedance measurements of the human body. Am J Clin Nutr 1985;41:810–7.
[27] Szczepaniak LS, Nurenberg P, Leonard D, et al. Magnetic resonance spectroscopy to measure hepatic triglyceride content: prevalence of hepatic steatosis in the general population. Am J Physiol Endocrinol Metab 2005;288:E462–8.
[28] Marti B, Tuomilehto J, Salomaa V, et al. Body fat distribution in the Finnish population: environmental determinants and predictive power for cardiovascular risk factor levels. J Epidemiol Commun Health 1991;45:131–7.
[29] Kotronen A, Westerbacka J, Bergholm R, et al. Liver fat in the metabolic syndrome. J Clin Endocrinol Metab 2007;92:3490–7.
[30] Kadish AL, Sternberg J. A new and rapid method for the determination of glucose by measurement of rate of oxygen consumption. Clin Chem 1968;14:116–31.
[31] Stenman UH, Pesonen K, Ylinen K, et al. Rapid chromatographic quantitation of glycosylated haemoglobins. J Chromatogr 1984;297:327–32.
[32] Friedewald WT, Levy RI, Fredrickson DS. Estimation of the concentration of low-density lipoprotein cholesterol in plasma, without use of the preparative ultracentrifuge. Clin Chem 1972;18:499–502.
[33] Chalasani N, Younossi Z, Lavine JE, et al. The diagnosis and management of non-alcoholic fatty liver disease: practice guideline by the American Gastroenterological Association, American Association for the Study of Liver Diseases, and American College of Gastroenterology. Gastroenterology 2012;142:1592–609.
[34] Matthews DR, Hosker JP, Rudenski AS, et al. Homeostasis model assessment: insulin resistance and beta-cell function from fasting plasma glucose and insulin concentrations in man. Diabetologia 1985;28:412–9.
[35] Lin LI. A concordance correlation coefficient to evaluate reproducibility. Biometrics 1989;45:255–68.
[36] Springer F, Machann J, Claussen CD, et al. Liver fat content determined by magnetic resonance imaging and spectroscopy. World J Gastroenterol 2010;16:1560–6.
[37] Cowin GJ, Jonsson JR, Bauer JD, et al. Magnetic resonance imaging and spectroscopy for monitoring liver steatosis. J Magn Reson Imaging 2008;28:937–45.
[38] Piekarski J, Goldberg HI, Royal SA, et al. Difference between liver and spleen CT numbers in the normal adult: its usefulness in predicting the presence of diffuse liver disease. Radiology 1980;137:727–9.
[39] Nomura F, Ohnishi K, Ochiai T, et al. Obesity-related nonalcoholic fatty liver: CT features and follow-up studies after low-calorie diet. Radiology 1987;162:845–7.
[40] Wieckowska A, McCullough AJ, Feldstein AE. Noninvasive diagnosis and monitoring of nonalcoholic steatohepatitis: present and future. Hepatology 2007;46:582–9.